Non-Contact Scour Monitoring System for Highway Bridges

Sudhagar Nagarajan, Ph.D.

Associate Professor

Civil, Environmental and Geomatics Engineering

Florida Atlantic University

M. Arockiasamy, Ph.D., P.E., P.Eng., Fellow ASCE

Professor

Civil, Environmental and Geomatics Engineering

Florida Atlantic University

Boca Raton, FL 33431

Contract: BDV27-977-16

Final Report

Submittal Date November 2020

DISCLAIMER

TECHNICAL REPORT DOCUMENTATION PAGE

1. Report No.	2. Government Accession No.	3. Recipient's Catalog No.

4. Title and Subtitle	5. Report Date
Non-Contact Scour Monitoring for Highway Bridges	November 2020
	6. Performing Organization Code

7. Author(s)	8. Performing Organization Report No.
Sudhagar Nagarajan and Madasamy Arockiasamy	

9. Performing Organization Name and Address	10. Work Unit No. (TRAIS)
Florida Atlantic University, Civil, Environmental and Geomatics Engineering, 777 Glades Road, Boca Raton, FL 33431	
	11. Contract or Grant No.
	BDV27-977-16

12. Sponsoring Agency Name and Address	13. Type of Report and Period Covered
Florida Department of Transportation 605 Suwannee Street, MS 30 Tallahassee, FL 32399	Final Report. Jun 2019- Nov 2020
	14. Sponsoring Agency Code

15. Supplementary Notes

16. Abstract

The most common cause of bridge failures in the United States is from floods scouring bed material around bridge foundations. Bridge scour due to hydraulic forces accounts for 52% of bridge failures. Increasing occurrences of flood events and an increase in their magnitude will likely result in greater instances of scour damage to bridges. A significant number of existing bridges across the nation are not adequately designed or maintained in relation to scour vulnerability under extreme flood events and are at risk of premature end of service life. This research demonstrated a potential non-contact green laser-based scour monitoring technique that is safer and quickly deployable. The research explored the feasibility of the approach in laboratory and field conditions where water turbidity conditions allow. The methodologies and mathematical model to implement non-contact scour monitoring are presented in the report along with the results from experiments.

17. Key Word	18. Distribution Statement
Scour, Green laser, Non-contact techniques	No restrictions

19. Security Classif. (of this report)	20. Security Classif. (of this page)	21. No. of Pages	22. Price
Unclassified	Unclassified	40	

Form DOT F 1700.7 (8-72)   Reproduction of completed page authorized

ACKNOWLEDGMENTS

EXECUTIVE SUMMARY

Local scour poses potential damage to the bridge piers. Although researchers have developed instrumentation for scour detection around bridge piers, the current state-of-the-art practice relies on visual inspection by divers. As a potential alternative to the traditional methods, this research explored the possibilities of using non-contact and remote sensing-based laser ranging technique for scour mapping and monitoring. This research report summarized the existing methodologies along with required mathematical models, laboratory and field-based experiments.

The first stage of the project analyzed the existing literature on scour and instrumentation to measure its rate. Then, the research continued exploring the factors affecting the demonstrated green laser-based non-contact measuring system, including turbidity and refraction correction. As a non-contact technique, green laser shot from above water level will travel through both air and water mediums and requires refraction correction to be applied to the derived topography. Scour is the process that typically occurs around the bridge piers which will require the green laser system to move around to acquire a 360° view of the submerged structure. Hence, this research demonstrated the necessary mathematical models to perform direct georeferencing.

The second stage of the project explored the feasibility of the developed research methodology by laboratory and field experiments. The laboratory setup included developing a scour hole based on published literature. The ability of the green laser to map the scour hole dimensions under varying turbidity conditions is demonstrated and presented in the report. Finally, the research team performed field testing on railroad and highway bridges in static and stop and go modes to demonstrate the typical procedure to retrieve underwater topography and scour using a green laser mapping system along with its limitations.

TABLE OF CONTENTS

LIST OF TABLES

LIST OF FIGURES

1 INTRODUCTION

Scour is a major factor that can affect the structural stability of bridges. Scour is mainly caused by the process of erosion and sediment transportation around submerged bridge piers or abutments. This permanent or temporary transportation of soils can be due to several natural and artificial factors such as the nature of bed materials (e.g., gravel, sandstone and shales), flooding due to heavy rainfall, sudden increase in the water current, and increased boat traffic. The other environmental conditions such as temperature and turbidity of water also influence the rate of the scouring process. Bridge washouts are due to scour and stream or river instability processes and are preventable. A field example of a bridge pier tipping due to scour and bridge washout is shown in FIGURE 1-1(1).

FIGURE 1-1. Example of a bridge washout due to stream instability and or scour (1)

One of the largest contributors to the risk exposure of bridges is reported to be scour from moving water, combined with earth flows, slides, and land use change within a catchment, which can lead to increased quantities of floating debris in the water. Factors like runoff from watershed, sediment delivery, and sediment transport capacity to the channel can also influence the scour process (2)(3). Excessive scour is a critical problem that is typically handled by enforcing design requirements that make the submerged structures more resilient. Bridge owners have adopted various techniques to regularly monitor the scour process and perform retrofitting and rehabilitation as necessary.

Among the existing methods for scour monitoring, visual inspection by divers has been the standard practice. Visual inspection is time consuming, unsafe, laborious, and less cost effective. Several alternative methods have been presented in Prendergast and Gavin (4) that require the sensors to be installed underwater and near the structure of interest. Such methods have high installation cost and produce only limited information of the scour. Multi-beam sonar-based methods can provide multiple samples of the scour over an extended area of riverbed, but sonar devices have to be deployed on the water surface using a manned or unmanned floating platform. In addition, the beam width of the acoustic system is typically high; hence, capturing

small undulations due to scour is not possible. Therefore, this research proposes a method of using green laser for scour monitoring that is non-contact, accurate, fast and provide high resolution data.

This research used laser ranging sensor with the signal wavelength in the green spectrum (Approx. 500 nm) of Electro Magnetic Radiation (EMR) for underwater scour monitoring. This includes developing methodologies to use green laser system on a static or mobile platform like truck, boat, USV (Unmanned Surface Vehicles) and UAS (Unmanned Aerial Systems) to map the condition of bridge substructure over the waterways. The developed methodologies are tested using laboratory and field experiments to study the feasibility.

2 BACKGROUND

2.1 NATURE OF SCOUR PROCESS

Scour is defined as the erosion and removal of material from the bed and banks of streams due to flowing water. Scour occurs in three main forms, namely, general scour, contraction scour and local scour. General scour occurs naturally in river channels and includes the aggradation and degradation of the riverbed that may occur as a result of changes in the hydraulic parameters governing the water channel. It relates to the evolution of the waterway and is associated with the progression of scour and filling, in the absence of obstacles. Contraction scour occurs as a result of the reduction in the channel's cross-sectional area that arises due to the construction of structures such as bridge piers and abutments. It manifests itself as an increase in flow velocity and resulting in bed shear stresses, caused by a reduction in the channel's cross-sectional area at the location of a bridge. The increasing shear stresses can overcome the channel bed's threshold shear stress and mobilize the sediments. Local scour occurs around individual bridge piers and abutments (4). Downward flow is induced at the upstream end of bridge piers, leading to much localized erosion in the direct vicinity of the structure (FIGURE 2-1).
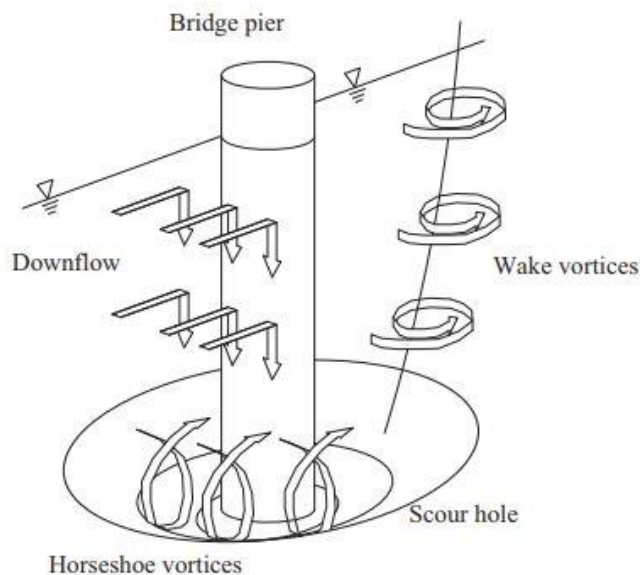
FIGURE 2-1. Scour process (4)

Horseshoe vortices develop due to the separation of the flow at the edge of the scour hole upstream of the pier and result in pushing the down-flow inside the scour hole closer to the pier. Horseshoe vortices are a result of initial scouring and not the primary cause of scour. Furthermore, separation of the flow at the sides of the pier results in wake vortices. Local scour depends on the balance between streambed erosion and sediment deposition. Clear-water scour is the term given to describe the situation when no sediments are delivered by the river whereas live-bed scour describes the situation where an interaction exists between sediment transport and

the scour process. The presence of live-bed conditions leads to greater ultimate scour depths than in clear-water conditions.

The equation given by HEC-18 (5) is widely used nationally and other parts of world for scour depth estimation.

$z = 2K_sK_\theta K_f\ K_A\ (b/y)^{0.65}\ yF_m^{0.43}$------Equation 1

Where z is the local scour; y is the flow depth, b is the pier width, Fm is the Froude number and K_s, K_θ, K_f, K_A represent various correction factors.

2.1.1   *Factors Affecting the Rate, Shape, and Magnitude of Scour*

The factors affecting the scour depend on the type of scour (6). For contraction scour, the main factor is the magnitude of constriction by which the waterway becomes narrower. The type of vegetation in the catchment area as floating woody debris from the plantation also narrows the waterway by clogging. The main factors affecting the local scour are geometry of the bridge, the type, shape and size of the pier, and the orientation of the pier with respect to the normal flow of water etc. The armor phenomenon also affects the local scour. When the finer bed materials are eroded, an armor layer is formed by the coarser materials; but deeper scour holes are expected when the flow exceeds the mobility threshold for the coarser materials. In the case of general scour, the main factors involved are natural and human activities. The natural factors are geomorphology of the catchment area, riverbed characteristics and natural disasters such as earthquake induced riverbed uplift and human activities involving construction of hydraulic structures and riverbed mining etc. The scour process also depends upon the properties of bed material. The mechanism of scour is quite different in the case of non-cohesive and cohesive sediment. The properties of individual particle influence the erosion threshold conditions in non-cohesive sediment, whereas, in the case of cohesive sediment, electrochemical bonding between individual particles is the deciding factor for erosion. The surface physicochemical forces in cohesive sediments are more important factors in comparison to weight of the particles that affect the possibility of erosion. These physicochemical forces vary with degree of saturation, drainage conditions, clay percentage etc. A very large number of researchers worked on scour in non-cohesive sediments but scour phenomenon in cohesive sediment still needed attention for active research (7). Also, in the case of gravel as bed material the magnitude of scour depth is changed due to bed roughness. The bed roughness is changed due to presence of gravel which results in different effects of gravel size and gradation on scour depth in comparison to sand as bed material. The change in bed roughness effect, the vortex flow around the obstruction and also mobility of bed material is different in case of sand and gravel. Generally, the scour depth in gravel bed is more than in sand as bed material (8).

2.2   CURRENT STATE OF PRACTICE AND LIMITATIONS

Considering the importance of assessing the scour conditions, State DOT (Department of Transportation) and railroad agencies have developed condition assessment procedures for its underwater infrastructure. The frequency of condition assessment is decided based on the scour

criticality of the bridge structure which ranges from 1-5 years. The standard way of checking the scour condition for the bridge owners is by visual inspection (9). This is typically achieved by diving in the water and using basic tools like metal tapes or rulers. Despite being a standard approach, there are major limitations with visual inspection in terms of labor, safety, reliability and cost. The hostile conditions in the deep-water cause safety concerns for the divers. The limited visibility conditions also pose challenges in the reliability and objectivity of the measurements. In order to overcome the limitations of visual inspections by the divers, various instrumentations have been used in the last several decades (10). Among them, Prendergast and Gavin (4) categorize the scour monitoring devices as single-use devices, radar devices, gravity sensors, sound wave devices, and electrical conductivity devices.

2.2.1   Existing Scour Monitoring Instrumentation

A range of instruments have been developed to monitor the formation of scour holes (4). Single-use devices consist of float-out devices and tethered buried switches that can detect scour at their locations of installation. These devices are installed vertically in the riverbed, near a pier or abutment of interest and work on the principle that when the depth of scour reaches the installation depth of the device, they simply float out of the soil. When the device changes from a vertical orientation to a horizontal one, an electrical switch triggers, which can indicate to a data acquisition system that the device is no longer in the ground and that the scour depth has reached its elevation. Pulse or radar devices utilize radar signals or electromagnetic pulses to determine changes in the material properties that occur when a signal is propagated through a changing physical medium. This typically occurs at a water-sediment interface, and thus, this type of device can detect depth of scour at a particular location. Fiber-Bragg grating sensors are a form of piezo-electric device. These types of sensors operate based on the concept of measuring strain along embedded cantilever rods to generate electrical signals, which can indicate the progression of scour along the rod. Buried or driven rod systems work on the principle of a manual or automated gravity-based physical probe that rests on the streambed and moves downward as scour develops. A number of devices have been developed that use sound waves to monitor the progression of scour holes. They work on the same principle as devices that use electromagnetic waves, in that waves are reflected from materials of different densities, thus establishing the location of the water-sediment interface. Electrical conductivity devices use the differences in the electrical conductivity of various media to determine the location of the water-sediment interface. They work on the principle of measuring an electrical current between two probes.

Single or multi-beam sonar is a sound wave-based active ranging technique that can be used to determine the depth of the water column over the stream or riverbed. Hence, these echo sounders with single or multi-beam capability have been widely used for bathymetric applications. There are several commercial-grade echo sounders available in the bathymetry and hydrographic surveying market that have been used for scour monitoring (10). The single beam echo sounder can give depth of the water over stream or riverbed at a single location at a time. Due to its portability, the device can be moved around to sample multiple points around the scour-critical structures. This is supported by positioning systems such as Global Navigational Satellite System (GNSS) receivers. While echo sounders are used in conjunction with a GNSS receiver, the measured depth can be associated with an absolute coordinate system such as latitude and longitude or local map frame. Multiple depth observations along with 2D positions

5

from GNSS receivers can be used to reconstruct a 3D model of the scour profile. The major limitations of this approach are noisy returns of echo sounders and wide beam width that limits the ability to capture the exact shape of scour. In the areas where the water is completely clear, photogrammetry has been used for scour mapping (11). These scour monitoring instruments often require expensive installation and maintenance and can also be susceptible to debris damage during flooding. The interpretation of data from these instruments can also be time-consuming and difficult. Research is on-going in developing non-intrusive methods to detect local scour and monitor scour development.

3   GREEN LASER-BASED SCOUR MONITORING

The existing scour monitoring techniques have limitations in providing sufficient number of samples on the scour surface with less cost, labor, and time. The detailed reconstruction of scour is important to understand the immediate, near future, and long-term implications on the structural stability of the submerged structures. Hence this study uses a non-contact, green laser based ranging technique that can provide accurate representation of the scour by sampling it with thousands of points within a few seconds.

The commercial laser scanners use either infrared or green wavelength lasers. The spectral properties of water cause infrared wave lasers to be absorbed mostly, hence produces minimal to no reflection or scattering. Therefore, infrared laser is not suitable for underwater applications. This research demonstrates a methodology to use green laser for underwater scour monitoring. Green laser with wavelength of around 500 nm can penetrate through the water surface and hit the river/stream bed of the waterbody and reflect back to the receiver in the laser scanner. By this process, the laser pulse travels through multiple mediums and make several interactions with the surface. When laser is transmitted from the scanner, it travels from the air medium to water which causes refraction on its refraction plane and reaches the bed of the waterbody. Then the laser pulse typically goes through a diffuse scattering (i.e., scattering in all directions). The scattered or reflected pulse in the angle equal to the incident angle reaches the receiver located at the laser scanner. The geometry of this ranging principle is shown in FIGURE 3-1. The figure and notations are adapted from Smith et al (12) and Plenner (13).

Green lasers have been widely used for bathymetric applications by the mapping community through airborne missions. However, such systems are extremely bulky, expensive, less dense and hence not suitable for close range applications like local scour mapping where higher sampling is required. For a close-range mapping, green lasers have been used for various hydrologic and sediment mapping applications. Hodge et al. (14) used green laser to map fluvial sediment surfaces. Smith et al. (12) used green laser to get high resolution structure and particle size data for gravel beds to better understand the interaction of bed roughness with near-bed flow hydraulics, sediment entrainment, transport and deposition. Smith et. al. (12) and Plenner (13) developed a mathematical model using green laser to map hydraulic and fluvial environments. The proposed research will develop methodologies to use multi-platform green laser for underwater substructure scour of railroad/highway bridges.

Water clarity of a water column is described by its absorption and scattering properties which ultimately limit the measurement of water column depth. The most important factor in using green laser for underwater applications is water clarity (15). The performance of laser bathymetric systems is often described in terms of Secchi depth which is a measure to determine the water clarity by using a white or black and white disk. The Secchi depth is the depth that a human eye can see the disk through water medium. The high power and large beam divergence can help the laser to penetrate up to 3 times the Secchi depth (16). The Secchi depth alone cannot predict the performance of a laser sensor's ability to map as the diffuse attenuation coefficient varies with the scattering-to-absorption ratio of the water (17).

Turbidity is a measure of water clarity that allows the light to pass through it (18). Turbidity and water clarity are inversely related. Similarly, turbidity and Secchi depth are also inversely proportional (19). Brando et al (20) discuss the factors that affect turbidity. Some of them include sand, silt, mud, seagrass and macroalgae in water. The other factors include chlorophyll, Colored Dissolved Organic Matter (CDOM), and non-algal particles. These are the factors that influence the turbidity of a water body, which in turn, influence the propagation and trajectory of green laser. If the water is too turbid, or has a high fraction of suspended sediments, bubbles, or organic material, the volume backscatter will be greater than the bottom return and no depth can be determined.

3.1   REFRACTION CORRECTION MODEL

When the green laser is transmitted from a sensor that is above water, it travels through the mediums of air and water before it can come back to the receiver. Through this process, the laser will get refracted. The amount of refraction is dependent on incident angle of water medium. FIGURE 3-1 illustrates the refraction of green laser in water medium (21).

$$X_r = R_r \sin \emptyset_w \qquad \text{---Equation 2}$$

$$Y_r = R_r \cos \emptyset_w \qquad \text{---Equation 3}$$

$$Z_r = \frac{1.33 * \cos \theta_w (R_r - R_w)}{\sin \theta_a} + Z_w \text{ ---Equation 4}$$

Where, $R_w = Z_w * \tan \theta_a$ $R_r = \frac{R - R_w}{1.33^2} + R_w$

θ_a -incident angle of laser pulse, $\emptyset_w$ - azimuth of the laser pulse, θ_w - refraction angle, (X_r, Y_r, Z_r) coordinates of water bed after refraction, Z_w – water level height.
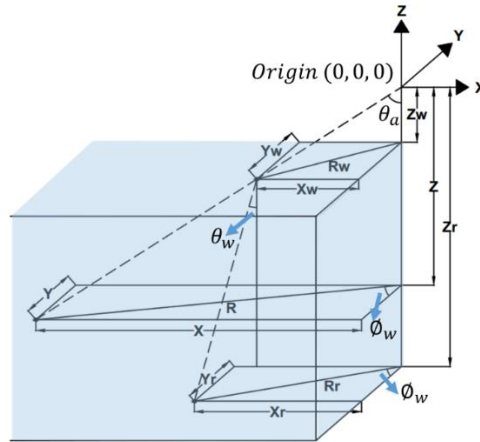
FIGURE 3-1. Schematic representation of applying refraction correction for underwater scanning

3.2 DEVELOPMENT OF REGISTRATION PROCEDURE FOR A MOBILE PLATFORM

When a mobile platform is used to derive scour dimensions around the pier, it is optimal to use a georeferencing procedure to visualize the scour depth. Hence, the water depth derived from laser scanner will need to be converted to 3D coordinates with respect to a fixed coordinate frame such as earth reference frame. The following mathematical model summarizes the direct georeferencing technique to derive 3D coordinates of scour hole using the green laser sensor mounted on a mobile platform.

3.2.1 Georeferencing Model

The green laser can be used on a static platform such as the one mounted on a tripod. However, such a static station limits the coverage of the complete scour profile, hence multiple stations are required. In order to overcome that limitation, a Mobile Mapping System (MMS) can be used. The MMS will have a green laser scanner mounted on a mobile platform such as boat, truck, Unmanned Surface Vehicle (USV) and UAS to acquire complete 360-degree view of the scour. This requires additional georeferencing sensors such as GNSS (Global Navigational Satellite System) and IMU (Inertial Measurement Unit). The following formulas adapted from Moafipoor et al (22) are used to derive the bathymetric elevations from green laser mounted on a multi-sensor mobile platform (FIGURE 3-2).
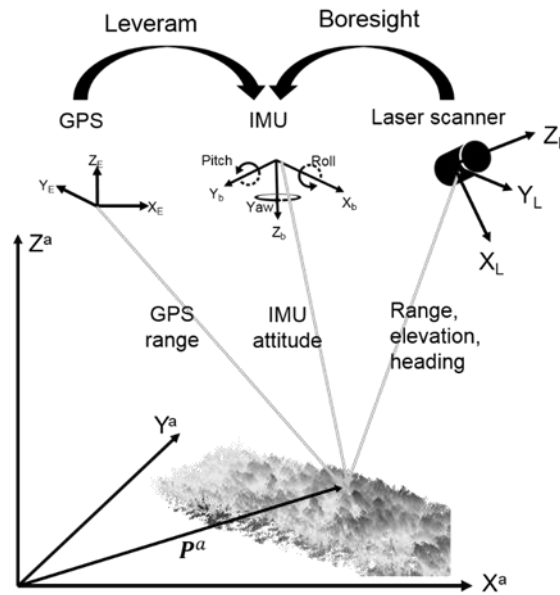
FIGURE 3-2. Mounting of different sensors in MMS

The coordinates of the bathymetric points computed from a sensor (after correcting for refraction) in a mobile platform is given by,

$$P^a = P_b^a + R_n^a R_b^n \left(R_L^b p_k + \Delta T_L^b \right) \text{---Equation 5}$$

where,

P^a—Coordinate of the captured point in the arbitrary a-frame of the laser scanner,

P_b^a—IMU position in the a-frame (Note that this requires accounting for level-arm offset between IMU and GPS sensor)

λ_i, φ_i are geodetic coordinates of P^a

R_b^n — Rotation matrix from body frame to local navigation frame,

R_L^b—Rotation matrix from LIDAR sensor frame to IMU (b-frame)—boresight rotation matrix

p_k—Coordinate of the point in LIDAR sensor frame (as recorded by the sensor)

ΔT_L^b—Offset between LIDAR sensor frame and the IMU—boresight translation.

R_n^a — Rotation matrix defined between local navigation frame (n-frame) and a-frame

$$R_n^a = \begin{bmatrix} -\sin(\lambda_i) & -\sin(\varphi_i) * \cos(\lambda_i) & \cos(\varphi_i) * \cos(\lambda_i) \\ \cos(\lambda_i) & -\sin(\varphi_i) * \sin(\lambda_i) & \cos(\varphi_i) * \sin(\lambda_i) \\ 0 & \cos(\varphi_i) & \sin(\varphi_i) \end{bmatrix}$$

4 LABORATORY TESTING

As demonstrated in Nagarajan et al (21), the theory that was adapted in developing lab scour holes is discussed below:

Cylindrical Pier in a Single Foundation Stratum: Based on the extensive published literature on pier scour at a cylindrical pier in a single stratum of non-cohesive foundation material, the basic variables are identified and shown in FIGURE 4-1. The functional relation between the depth of local scour, y_s, and the variables can be stated as

y_s= function [flow (ρ, μ, V,y, g), bed material (D, σ_g, ρ_s, V_c), pier (a, b, Ω, θ), time (t) --- Equation 6

where ρ and μ = fluid density and molecular viscosity respectively; V = depth averaged velocity of approach flow; y = approach flow depth; and g = gravity acceleration; V_c= critical shear velocity for bed sediment entrainment; D and σ_g = median size and geometric standard deviation of the foundation material particle size distribution; ρ_s = sediment density; and c = a parameter describing cohesiveness of the material; a = pier width; b = pier length; Ω = parameter describing the shape of the pier face (upstream side); θ = angle of the flow relative to pier alignment; and t = time
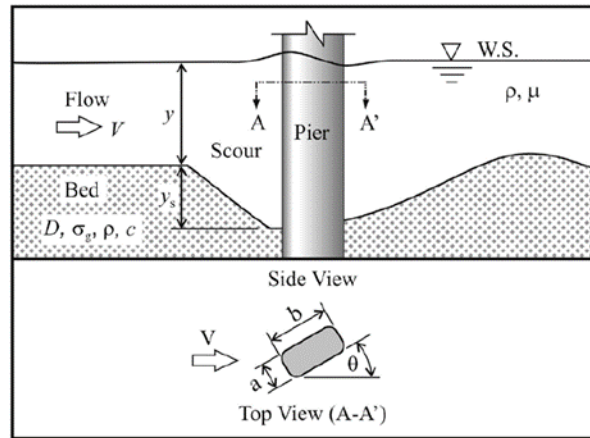
FIGURE 4-1. Variables influencing pier scour at a cylindrical pier (23)

Local Pier Scour Prediction: The equation used by Richardson et al., (24) for estimating the depth of local scour at piers accounts for additional parameter influences (25) and is given by

$y/a = 2.0\ K_1\ K_2\ K_3\ K_4\ K_W\{ y/a\}^{0.35}\ Fr^{0.43}$ ---Equation 7

where, $F_r = V/(gy)0.5$; and K_1, K_2 and K_3= adjustment factors accounting for pier nose shape, angle of attack of flow, and state of bed sediment motion, respectively. K_1 varies between 0.9 and 1.1, K_2 varies between 1.0 and 5.0, and K_3 varies between 1.1 and 1.3. The factor, K_4, is a correction factor for armoring by bed material size. K_W is the pier scour correction factor for wide piers.

Top width of Scour Hole: The top width of a scour hole in cohesionless bed material from one side of a pier or footing can be estimated from the following equation (26):

$W = y_s(\ K+\cot\theta)$---Equation 8

where: W = Top width of the scour hole from each side of the pier or footing, m

y_s = Scour depth, m (ft)

K = Bottom width of the scour hole, related to the depth of scour

θ= Angle of repose of the bed material ranging from about *30° to 44°*

The angle of repose of cohesionless material in air ranges from about 30° to 44°. Therefore, if the bottom width of the scour hole is equal to the depth of scour y_s *(K = 1)*, the top width in cohesionless sand would vary from 2.07 to 2.80 y_s. At the other extreme, if $K = 0$, the top width would vary from 1.07 to 1.8 y_s. Thus, the top width could range from 1.0 to 2.8 y_s. A top width of 2.0 y_s is suggested for practical applications.

Length of Scour Hole: Dimensional analysis has indicated scour length as a function of densimetric Froude number and inflow depth. Hence, measured relative (non-dimensional) scour lengths (L_s) are plotted against the calculated relative scour depths with inflow depth as variable parameter. Linear trend lines for the relative scour lengths for different inflow depths is assumed in the following form:

$L_s = C_2\,D_s + D_2$ --- Equation 9

Where, C_2 and D_2 are constants dependent on inflow depths. Relative scour length is given by

$L_s = \{3.958\ (h/b\ ) - 2.371\}\,D_s + \ \{- 2.649\ (h/b) +5.082\}$---Equation 10

Wherein, h = approach flow depth, b = pier diameter and D_s= relative scour depth (local equilibrium scour depth/pier diameter)

The simulated scour based on the above theory is tested using the developed green laser-based scour mapping methodology. The 3D scour hole dimensions and the soil bed topography were captured by the developed green laser system for simulated field conditions of water with varying sediment concentrations.

4.1   EXPERIMENTAL SETUP

Based on the theory discussed in the section above, the research team has designed a model scour hole with dimensions shown in FIGURE 4-2. Linear trend lines for the relative scour lengths are assumed for different inflow depths. The experiments are performed in a water pool (Bestway fast set) of 10-feet diameter and 30-in. depth with 1000-gal capacity. A 4-in. diameter PVC pipe simulating a circular pier was first installed at the center of the pool. The bridge pier scour hole was then set in position around the PVC pipe and the scour hole model held in place with coarse aggregate particles forming a 1:7.4 slope. The measurement of water depths in the pool using green laser was carried out with varying turbidity levels. The h value –water depth (shown in FIGURE 4-2) was changed from 8 inches to 16.5 inches based on the laser sensor's ability to see the scour hole under varying turbidity conditions.
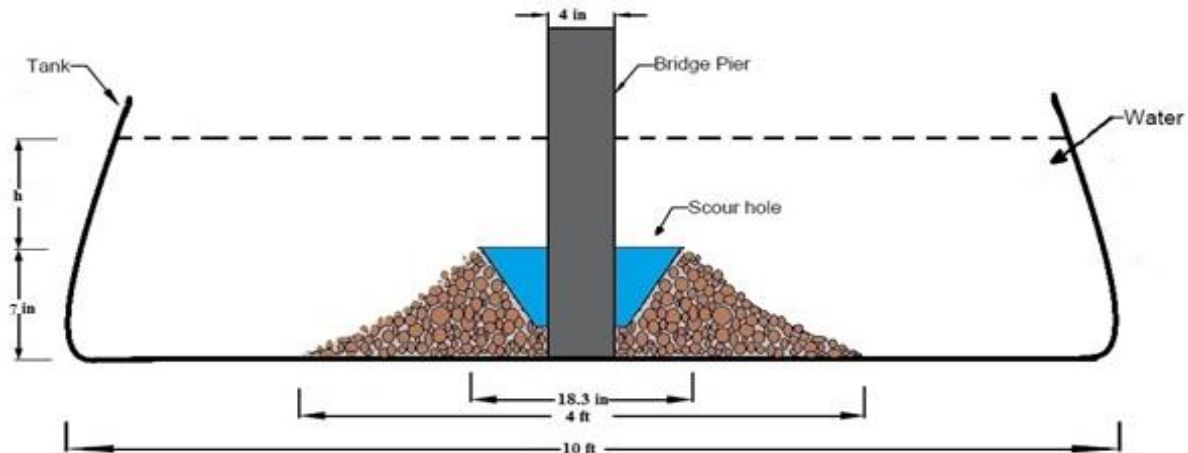
FIGURE 4-2. Scour hole model

4.1.1 Turbidity Conditions

Turbidity is a measure of water clarity which increases or decreases based on the amount of suspended particles in it. There are different materials that can cause turbidity, namely soil particles (clay, silt and sand), algae, plankton, microbes, etc.(27). As the depth of penetration of laser is based on the water clarity and turbidity conditions, it is essential to measure the turbidity to assess the suitability of a given laser medium. A turbidity meter measures the turbidity in terms of nephelometric turbidity units or NTUs. It is a measure of the intensity of light scattered at a 90° angle by the particles in the sample (27). Clear water has turbidity of less than 1 NTU, and about 80% percentage of fresh and coastal water bodies have turbidity 10 NTU or less (28) in a dry season.

4.1.2 Green Laser Sensor

Despite a handful of commercial bathymetric lidar systems available in the market, only a very few of them are suitable for drone or close-range applications. The ability of these systems to see the bed of waterbodies is typically given by Secchi depth. For lab experiments, an in-house Leica Scanstation 2 was used. Similar to commercial-grade bathymetric systems, Scanstation 2 uses a green laser with 532 nm wavelength. As compared to in-house laser systems, commercial bathymetric systems have better Secchi depth and mobile mapping capability and less range precision.

4.1.3 Calibration and Reference Model Generation

In order to compare the dimensions retrieved from various turbidity conditions, the 3D shape of the fabricated scour hole shown in FIGURE 4-3 is extracted with Leica Scanstation 2 in dry conditions. Performing scanning during dry conditions ensures underwater and turbidity condition do not influence geometric shape and dimensions of the scour hole. The retrieved

13

dimensions of the scour hole are shown in FIGURE 4-3 and FIGURE 4-4. This 3D model is used as a reference for all underwater experiments discussed in the sections below.
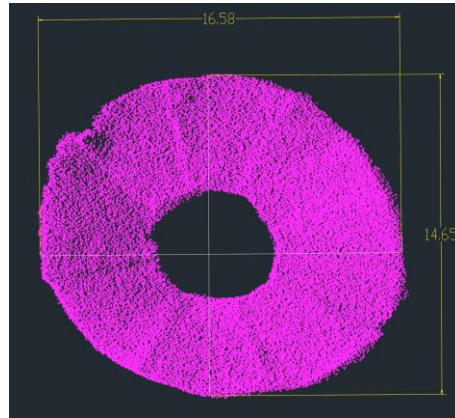

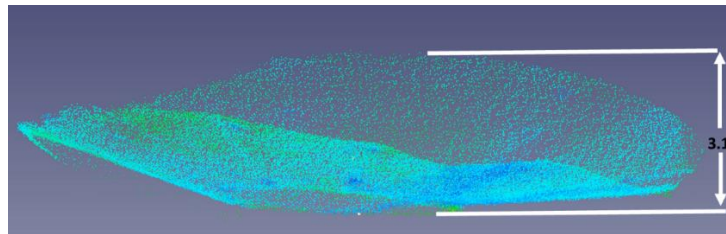**FIGURE 4-3. Dimensions of scanned scour hole without water (units are in inches)**

FIGURE 4-4. Depth of scanned scour hole (depth in inches)

4.2   EXPERIMENTS

Depending on the type, power and relative Secchi depth of the green laser system, the penetration depth and allowable turbidity conditions could vary. Hence, the experiments are designed only to validate the developed methodologies to reconstruct 3D scour hole model using a green laser sensor.

The experimental setup for underwater conditions is shown in FIGURE 4-5 where the laser scanner is mounted on a tripod on the sides of water tank, so it is clearly visible. As the simulated pier includes a part of scour hole from being seen by the laser scanner, two stations are needed to be able to capture full 360° of the scour hole and tank. Note that the locations of these stations are chosen in such a way the 360° view of the experimental setup could be acquired. For each station and trial discussed in the experiments below, the laser scanner is setup on the tripod. After horizontally leveling the equipment, it is connected through the data collection software Cyclone and 3D laser scan for the area of interest to be captured. The other scan parameters for the scan include minimum range, maximum range, minimum reflectance of laser pulse energy and point density. As for the experiments, 1 % percent reflectance of incident energy and the

point spacing of 5 mm at 15 feet range were used. These settings were fixed for all the trials discussed in the rest of the report. FIGURE 4-5 shows 2 of 5 targets used in the setup. The targets are setup in a way they are visible from both stations. These targets are used to register (tie) the 3D laser scans acquired from two stations.
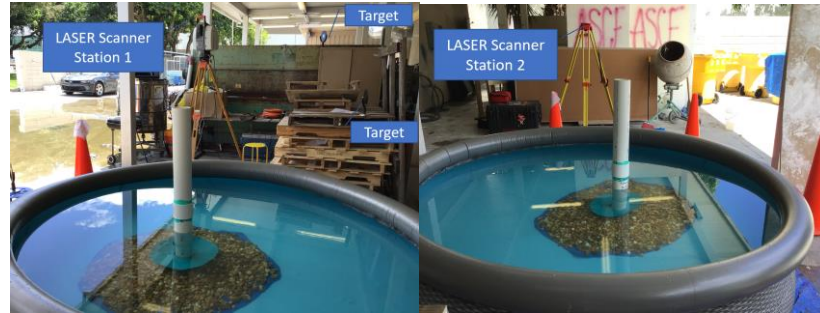

FIGURE 4-5. Laser scanner setup: station 1 (left); station 2 (right)

4.2.1 Trial 1: Turbidity 1.2 NTU

As changing the turbidity of the larger tank is a tedious task, the research team used a Bestway fast set pool shown in FIGURE 4-2 for the experiments. This setup had water depth of 20.5 inches everywhere and 16.5 inches at scour hole. The turbidity value of the water used in the setup is 1.2 NTU. The bed topography and the scour hole model were reconstructed based on the formulas and methodology discussed in earlier sections of the report. FIGURE 4-6 illustrates the 3D laser scan before and after refraction correction that was acquired from Station 1. FIGURE 4-7 shows the 3D scan of the tank and scour hole from the second scan station. After applying refraction correction of both stations, the data are registered by using the target to target registration technique. It is the process of 3D conformal transformation procedures by using common targets that are visible in both stations' data. The registration was performed using Leica Cyclone software. FIGURE 4-8 shows the dimensions of the scour hole retrieved after refraction correction. Note that these dimensions are measured with respect to same vertical and horizontal reference lines shown in FIGURE 4-3. The retrieved 3D point cloud of Trial 1 along with reference 3D point cloud of scour hole (shown in FIGURE 4-3) is displayed in FIGURE 4-8.
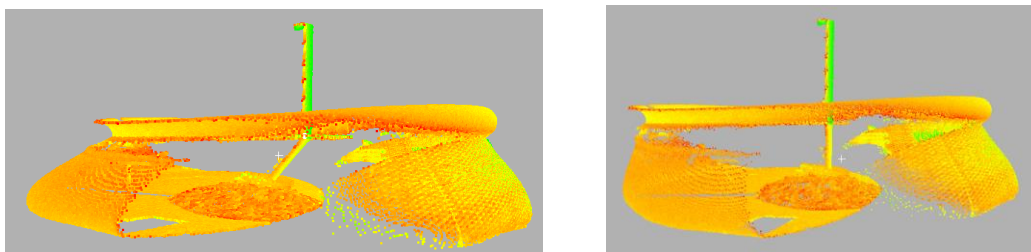

FIGURE 4-6. Trial 1 experimental setup: 3D laser scan before refraction correction (left); 3D laser scan after refraction correction (right)
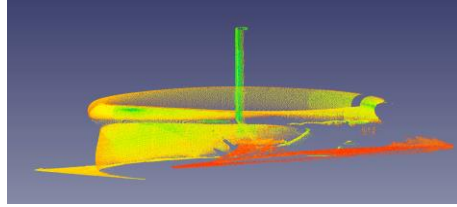
15

FIGURE 4-7. 3D reconstruction of Trial 1 experimental setup (station 2)
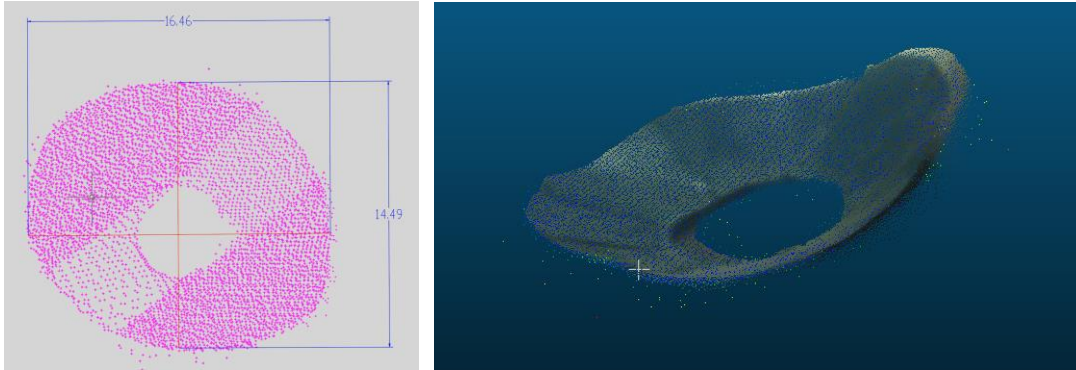
FIGURE 4-8. Retrieved scour model for Trial 1: Dimensions (left); 3D overlay (right)

4.2.2 Trial 2: Turbidity 3.9 NTU

This setup is exactly same as Trial 1: Turbidity 1.2 NTU except the turbidity level of the water is increased by adding kaolinite. The kaolinite used in the experiments have median particle size of 1.5 micron which easily suspends in the water. To increase the turbidity values gradually, a kaolinite mixed solution was added to the water. After mixing with the water, the turbidity level was checked. For this Trial 2, the turbidity came out to be 3.9 NTU. FIGURE 4-9 illustrates the 3D laser scans before and after refraction correction. As shown, both the bed topography and scour model could be reconstructed using the discussed methodology. The dimensions of the scour hole are retrieved with respect to the same reference lines shown in FIGURE 4-3 and FIGURE 4-8. The retrieved dimensions are discussed in TABLE 4-1 and TABLE 4-2.

FIGURE 4-9. 3D reconstruction of Trial 2 experimental setup: 3D laser scan before refraction correction (left); 3D laser scan after refraction correction (right)
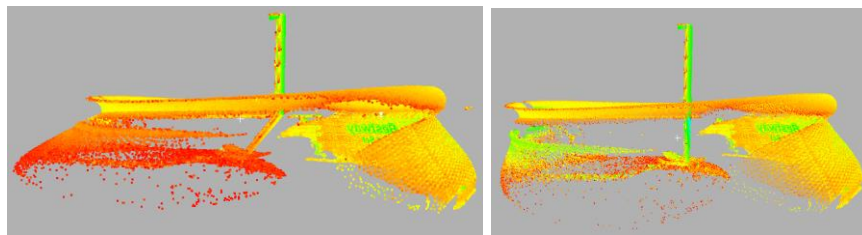
16

4.2.3   Trial 3: Turbidity 5.5 NTU

This setup used the same water pool and scour hole setup. But the water level was 12.5 inches near the scour hole and 16.5 inches everywhere else. The overall water level was reduced in this experiment to improve the stability of the tank. However, the turbidity level was increased to 5.5 NTU. FIGURE 4-10 illustrates the laser scans of this setup before and after refraction correction. Both the bed and scour hole topography could be reconstructed using the collected laser scans. The dimensions are measured with respect to the same vertical and horizontal lines used in other trials.

FIGURE 4-10. 3D reconstruction of Trial 3 Experimental setup: 3D laser scan before refraction correction (left); 3D laser scan after refraction correction (right)

4.2.4   Trial 4: Turbidity 6.4 NTU

The experiment was continued with increasing turbidity levels. For this *Trial 4* setup, the turbidity level was increased to 6.4 using the kaolinite solution. The water levels were kept to same as *Trial 3*. FIGURE 4-11 illustrates that the both underwater bed topography and scour hole could be recovered.

FIGURE 4-11. 3D reconstruction of Trial 4 experimental setup: 3D laser scan before refraction correction (left); 3D laser scan after refraction correction (right)

4.2.5   Trial 5: Turbidity 12.1 NTU

This setup used the same water pool but with turbidity of 12.1 NTU. As the turbidity values started to increase, the laser sensor used in the experiment could no longer see the bed

topography. Hence the water levels were decreased to 8 inches near scour hole and 12 inches everywhere else. Despite that, only the scour hole model could be recovered and not the bed topography. The point clouds of the scour hole before and after refraction correction are illustrated in FIGURE 4-12.
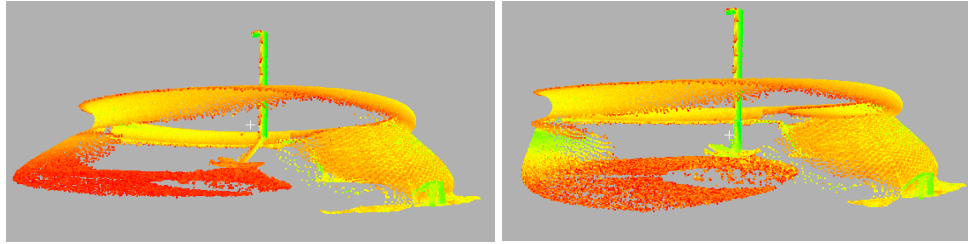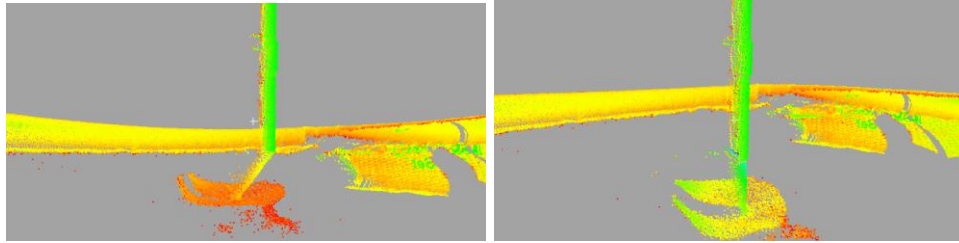

FIGURE 4-12. 3D reconstruction of Trial 5 experimental setup: 3D laser scan before refraction correction (left); 3D laser scan after refraction correction (right)

4.2.6   Trial 6: Turbidity 20.8 NTU

This was the last setup that was used in the laboratory. The water levels were kept same as

Trial 5: Turbidity 12.1 NTU, but the turbidity was increased to 20.8 using the kaolinite. As in the case of *Trial 5*, only the scour hole topography could be recovered. This is shown in FIGURE 4-13.
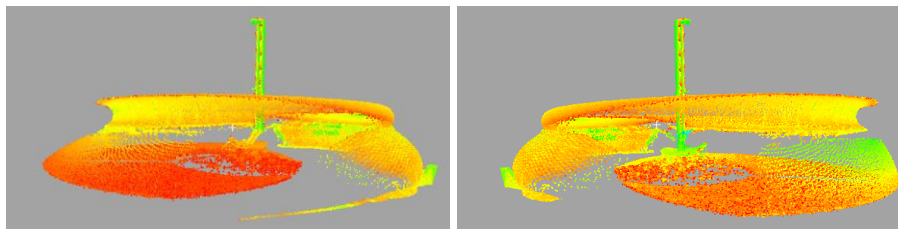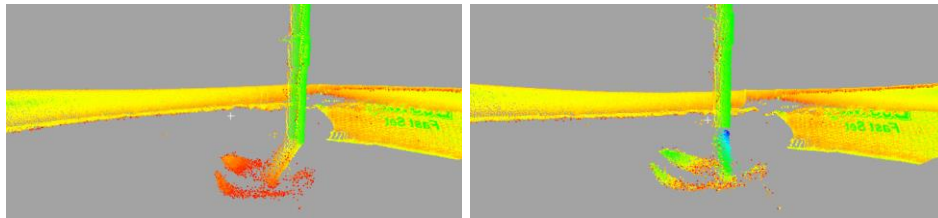

FIGURE 4-13. 3D reconstruction of Trial 6 experimental setup: 3D laser scan before refraction correction (left); 3D laser scan after refraction correction (right)

The dimensions of the recovered scour hole with respect to same vertical and horizontal reference lines for various trials are presented in TABLE 4-1 below. By considering the scour hole measurements without water as a reference, errors in width, length and depth are computed for each trial and the results are shown in TABLE 4-2.

TABLE 4-1. Dimensions of scour hole

Trial No	Turbidity (NTU)	Scour Width (inches)	Scour Length (inches)	Scour Height (inches)	Water Depth (inches)
Above water	N/A	16.58	14.65	3.10	N/A
1	1.2	16.46	14.49	3.01	20.1
2	3.9	16.4	14.41	2.97	20.3
3	5.5	16.4	14.72	2.99	16.5
4	6.4	17.1	14.46	2.95	10.8
5	12.1	17.11	14.4	3.09	12.4
6	20.8	16.3	14.4	3.09	12.4

TABLE 4-2. Errors in retrieved dimensions

Trial No	Width error (in.)	Length error (in.)	Height error (in.)
1	0.21	-0.16	-0.09
2	-0.18	-0.24	-0.13
3	-0.18	0.07	-0.11
4	0.52	-0.19	-0.15
5	0.53	-0.25	-0.01
6	-0.28	-0.25	-0.01
RMS	0.35	0.20	0.10

5 FIELD TESTING

The research team interacted with Florida DOT and the railroad industry partner CSX Transportation's Engineering Standards team to identify the bridges that will be suitable for field testing. The major criteria that were put forth for the selection were accessibility to the site and bridge, nominal depth, and turbidity conditions. From the handful of sites that were chosen, one each on railroad and highway bridges were used for field testing. This includes CSX railroad bridge SXG59.70 located in Miami-Dade County, crossing C-1W canal, and Florida DOT bridge located in Little Lake Worth, Palm Beach Gardens. The following subsections discuss the data collection procedure and results of each of the bridges separately.

5.1 RAILROAD BRIDGE – SXG59.70

5.1.1 Bridge Specifications

The SXG59.70 railroad bridge owned by CSX Transportation is located near SW 112th St, Miami, FL 33196 at latitude 25º39'39.2" N and longitude 80º28'43.8" W. The bridge has two spans of 14.8 ft. each and midspans of 20.9 ft. approximately. The research team visited the site twice, once for preliminaries and once for actual data collection respectively. FIGURE 5-1 and FIGURE 5-2 show the dimensions and pictorial view of the bridge, respectively. The average turbidity of the water is 0.45 NTU.
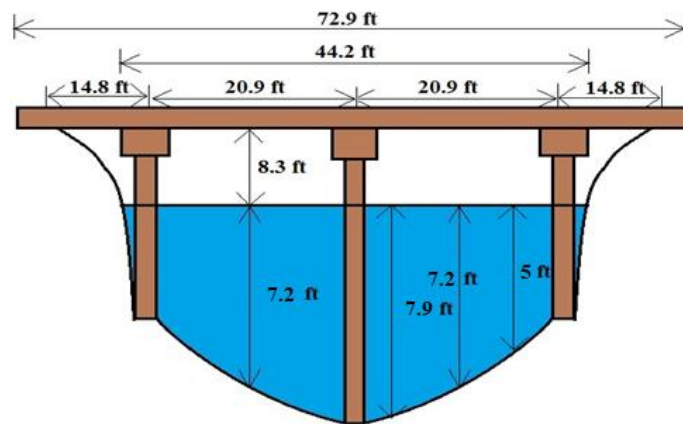

FIGURE 5-1. Railroad bridge – SXG59.70 dimensions and water depth

FIGURE 5-2. View of railroad bridge – SXG59.70

5.1.2 Data Collection

The data collection for the railroad bridge was performed using Leica Scanstation 2. Two static stations were setup on both sides of the canal berm to scan underwater near bridge piers. The minimum reflectance for the laser return was setup to 1% for each station. FIGURE 5-3 illustrate the collected 3D laser scans from both stations.
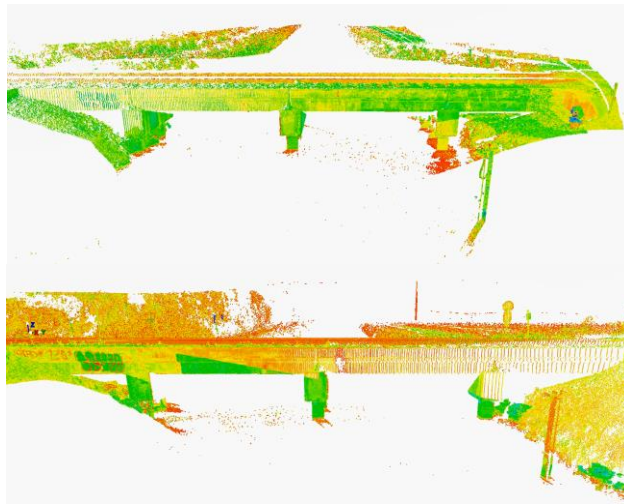
FIGURE 5-3. Laser point cloud: station 1 (top); station 2 (bottom)

5.1.3 Data Processing

This step of the process separates above and below water points for each of the scans and applies refraction correction to those points that are underwater. Note that the refraction correction is based on relative water level and inclination angle with respect to the origin of the laser scan. Hence, refraction correction is applied for both stations' scans independently. Then, the both stations' laser scans are registered and shown in FIGURE 5-4. FIGURE 5-5 shows the laser scan

21

for a small portion from station 1 and station 2 before and after refraction correction. The point cloud that is generated after refraction correction is shown in white in FIGURE 5-5.

FIGURE 5-4. Registered laser scans before refraction correction

FIGURE 5-5. Portion of laser point cloud before and after (white) refraction correction: station 1 (left); station 2 (right)

5.2 HIGHWAY BRIDGE – LITTLE LAKE WORTH

5.2.1 Bridge Specifications

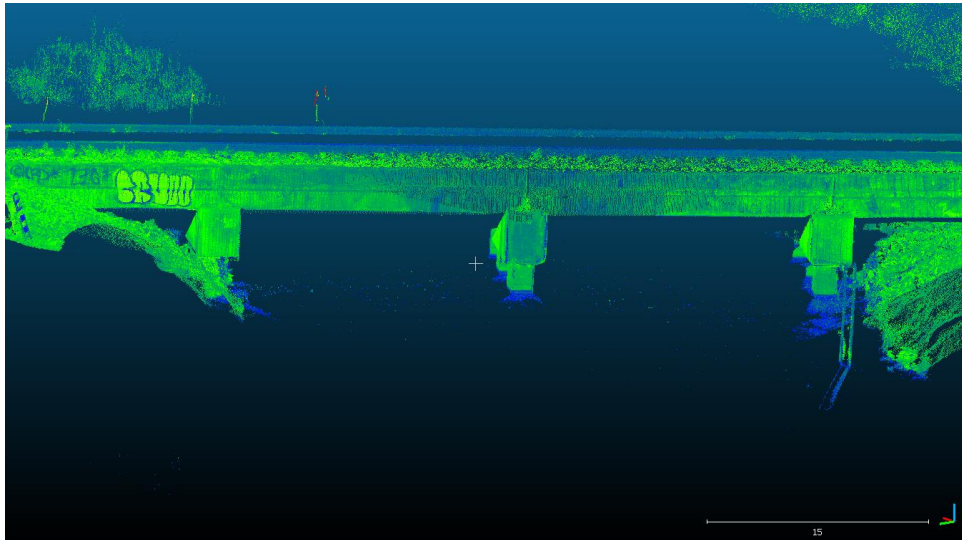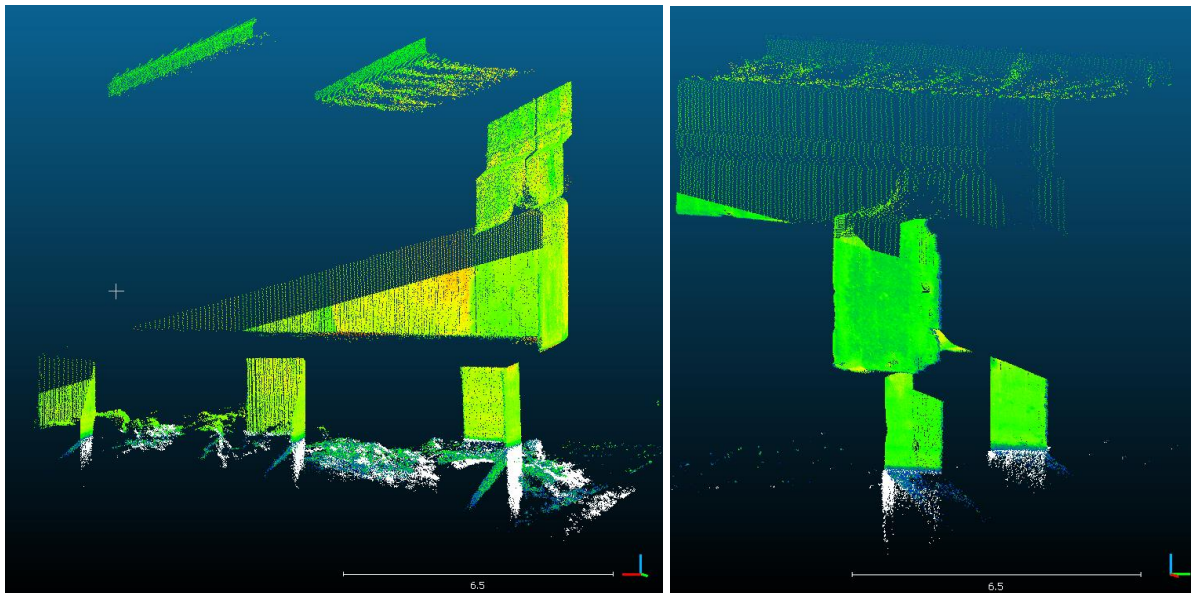The little lake worth bridge owned by Florida DOT (and maintained by its District 4) is located Near 11072-11078 Florida A1A, Palm Beach Gardens, FL 33408, and latitude 26°50'37.5"N longitude 80°03'27.1"W. The bridge spans Lake Worth lagoon, which is a tidal water body. The old Little lake Worth bridge was constructed in the year 1965. In 2006, Florida DOT District 4 has proposed to replace the old Little Lake Worth bridge as it was rated structurally deficient. The construction of new bridge that is 90 feet long and 57 feet and 7 inch wide was completed in 2012. The bridge is not skewed and has two spans of 26-feet and 6-inches and one midspan of 37-feet. The old bridge was 60 feet long, consists of two 15-foot long spans and a 30-foot long midspan, and is 43 feet and 9 inch wide. The new bridge is a reinforced concrete structure supported by pile bent substructures. FIGURE 5-6 and FIGURE 5-7 show the dimensions and pictorial view of the bridge respectively. FIGURE 5-8 display the topo-bathymetric data (29) acquired from airborne missions in the background of 2018 Orthoimage provided by Florida DOT (30).

The research team visited the site multiple times for reconnaissance, preliminary data collection and actual data collection. The turbidity of the water changed from 0.625 NTU to 1.740 NTU during this time with highest in the wet season and on the date (July 2020) of field data collection.
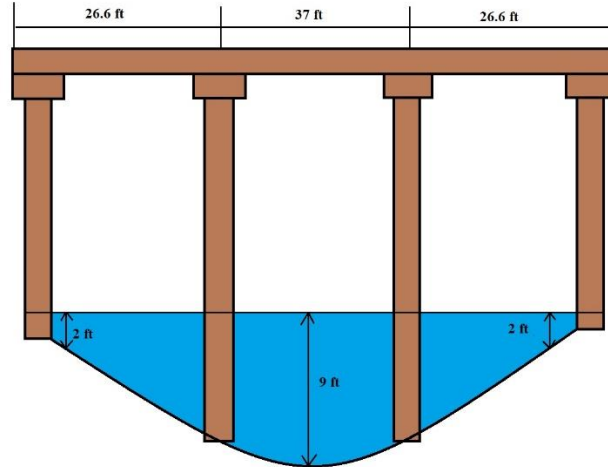

FIGURE 5-6. Lake Worth highway bridge – approximate dimensions and depth
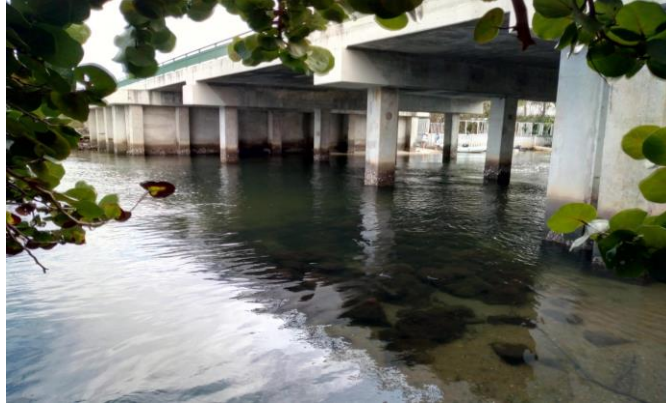
FIGURE 5-7. View of highway bridge: Little Lake Worth bridge
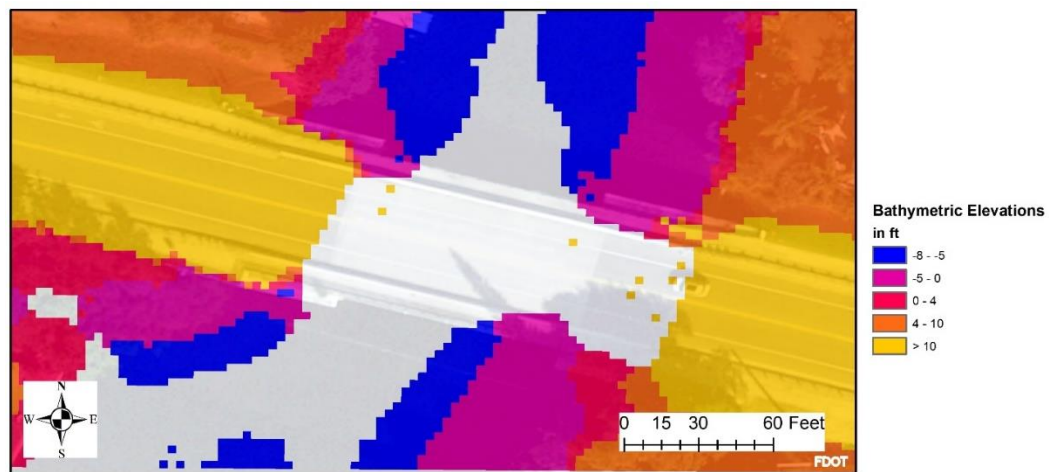
FIGURE 5-8. Topo bathymetric elevations of Little Lake Worth bridge

5.2.2   Data Collection

The data collection was performed on July 2nd, 2020 on a sunny day with temperature in low 90°s F. Leica Scan Station 2 was used for field testing. In order to move the equipment to multiple locations under the bridge for bathymetric measurements, the snooper truck owned by Florida DOT's District 4 was used. The snooper truck has a man-basket that can move forward, backward, above and below to get closer to different parts of the bridge. The laser scanner was setup on a tripod and the laser scanning data near bridge piers was collected in a stop and go mode. The stop and go mode collects data when the scanner is stationary, and no data is collected when the man-basket is in motion. The data was collected from 6 different stations mostly focusing on near the abutment due to higher turbidity that limited the water penetration of the laser scanner. The FIGURE 5-9 shows the setup and FIGURE 5-10 shows registered point cloud of all 6 stations. The water samples were collected from the top of water surface and the average turbidity came out to be 1.720 NTU.

24

FIGURE 5-9. Field data collection setup with snooper truck
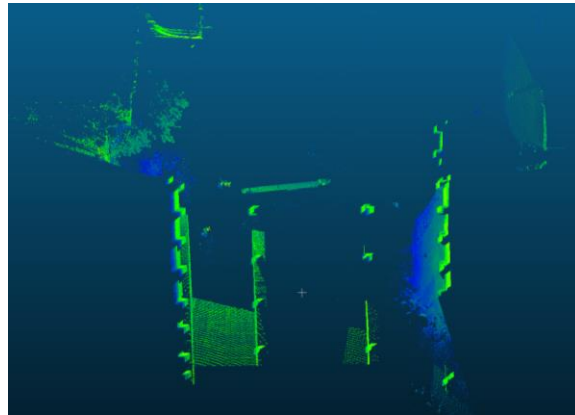
FIGURE 5-10. Lake Worth bridge data overview (oriented to north)

5.2.3 Data Processing

The laser scanning data collected for each station has points above and below water. The points that penetrated and refracted through water have to be corrected for refraction based on the inclination angle of the laser and water surface elevation. The process of separating above water and below water points was manually performed and refraction corrections were applied based on the water level elevation. With respect to the laser scanner that was on the basket, water level is not a constant due to water current and out of level tripod. Hence, the water level elevation is fitted as a plane by manually picking water level points on multiple locations. FIGURE 5-11 shows both above and below water points before refractions correction. FIGURE 5-12 displays the points after applying refraction correction.
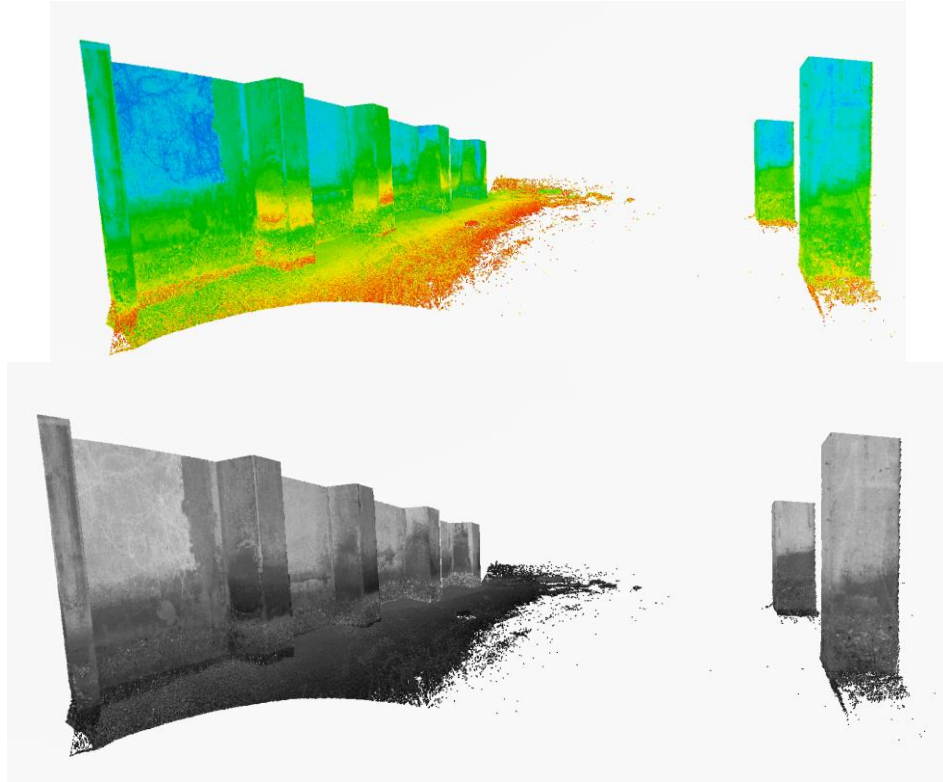
**FIGURE 5-11. Portion of green laser point cloud data: Display by hue intensity (top);
Display by intensity (bottom)**

FIGURE 5-12. Example point cloud before (green) and after (white) refraction correction

6   PROJECT SUMMARY AND CONCLUSIONS

The project investigators developed and studied the feasibility of non-contact scour monitoring technique using green laser. Despite the challenges in terms of the unavailability of laser scanner in the market that is suitable for higher turbidity conditions, the research has demonstrated the methodology and steps involved in using green laser for scour mapping applications.
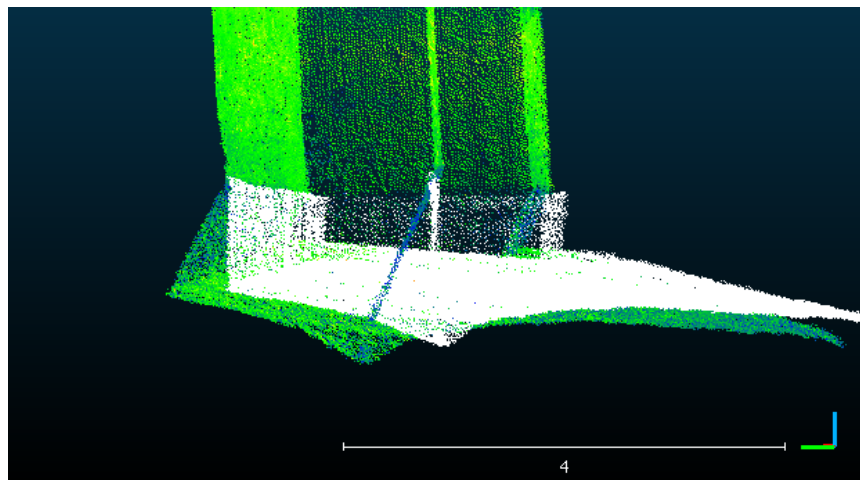
The project team expect that the project will be a useful resource for the drainage/bridge maintenance team to adopt this non-contact techniques where suitable conditions and equipment are available. In such as case, the typical sequence of field implementation will be as follows.

Step 1: The bridge maintenance engineer will study the turbidity conditions of the water using a turbidity meter. Then use the Secchi disk to measure the Secchi depth of the turbid water.

Step 2: Check the suitability of the green laser scanner owned by the bridge owner. If the laser scanner indeed is suitable based on the turbidity/Secchi depth, take it to the field.

Step 3: Based on the range of the equipment, deploy the green laser scanner in the field in static or mobile (snooper truck/boat/drone)

Step 4: Collect the data using the green laser around the bridge piers of interest.

Step 5: Apply refraction correction for the laser returns from underwater using the research methodology discussed in this report (*Section: Refraction Correction Model*)

Step 6: (Optional) If georeferencing sensors are used, perform georeferencing using the methodology discussed in the section *Development of Registration Procedure for a Mobile Platform* of the report.

6.1   PROJECT RESULTS

The project is implemented in two stages. Stage I of the project mainly focused on development of methodology to use multi-platform based bathymetric system for scour measurement. This includes deriving refraction correction procedures and development of registration methodology for multi-sensor platform. 3D concave shaped scour hole models were fabricated and tested under varying depth and turbidity conditions using the developed methodology. The results were compared with original dimensions to validate the feasibility of Green laser-based scour measurement methodology. Stage 2 of the project chose candidate bridges for field testing to implement the demonstrated methodology. The results of the field testing suggest that green laser-based scour measurement is feasible if appropriate instrumentation is used for the given water conditions.

6.2 CONCLUSIONS

This project demonstrated methodologies to quantitatively evaluate the scour of bridge pier foundations by utilizing static or mobile platform-based green laser bathymetry measurements. The discussed methodologies have the potential to make scour mapping feasible, quick, safe, and economical for bridge owners if suitable turbidity conditions exist. The green laser can generate high definition 3D riverbed topography that is suitable to map and monitor the development of scouring process.

The research developed the methodology which could be implemented in various steps along with the application of necessary mathematical models. Then, the feasibility of the methodology was first evaluated in a laboratory setup with simulated scour holes that were created based on published literature and the principles of similitude. The research further experimented with the techniques in the field using static and stop and go mode, respectively, for railroad and highway bridges. Both laboratory and field testing were performed using Leica Scanstation 2 green laser scanner.

The purpose of the laboratory experiments was to evaluate the feasibility of the demonstrated green laser-based scour monitoring system and methodology. The in-house green laser scanner was used to map the underwater scour and bed topography. For Trials 1-4 with turbidity values less than 6.4 NTU and bed depth 20.5 inches or less, both scour hole and the bed topography were mapped. As turbidity level increased, the ability of the laser scanner to see the bed topography also was reduced despite decreasing the depth to 12 inches. This indicates that for a given laser sensor, the penetration depth could change based on the turbidity levels. The errors shown in TABLE 4-2 attest to both resolution and the limitation of the laser scanner to capture the sharp edges (31), which limits the ability of the user to manually extract the exact dimensions of the scour hole from the point cloud. Though the laser scanner can extract highly precise geometric information, it has limitations in capturing the edges, unlike images. However, the real-world scour profiles are not likely to have sharp edges, unlike the one used in lab experiments. Despite that limitation, the RMS (root mean square) errors in the retrieved dimensions were 0.35 in., 0.20 in., and 0.1 in., in width, length, and depth, respectively. The lab experiments demonstrated the limitations of technology when the turbidity values started to increase. The increased turbidity caused excessive noise and ultimately affected the penetrability of the laser.

The field experiments produced underwater topography for the portion that has very shallow depth. In other parts, the laser could penetrate up to a maximum of 3 feet. Note that the depth penetration (also called as maximum surveyable depth) depends on a combination of hardware and environmental factors such as water clarity (turbidity), laser pulse energy, range, and laser inclination angle (15) (32). The results shown in FIGURE 5-5 demonstrate the feasibility of the project methodology to scan underwater and apply refraction correction under the conditions suitable for the given laser sensor. The experiment for the highway bridge used a stop-and-go method instead of the static mode that was adapted for the railroad bridge. The stop-and-go method enabled the laser scanner to go closer to the bridge piers. However, the higher turbidity conditions enabled the laser scanner to map the underwater bed topography only in the shallow areas near the bridge abutment. The maximum depth that could be extracted by the laser scanner through the experiments is about 2 feet. The current state-of-the-art systems that are commercially available can see the depth (up 30 feet) when clear water or less than 0.5 NTU turbidity conditions exist. As turbidity values increases to 8 NTU, the ability of the green laser

system will drastically reduce to 3 feet or even less, which limits the scope of green laser-based scour monitoring to only clear water and near-clear water conditions.

The research also studied the aspects of turbidity, Secchi depth, laser power, laser wavelength and range having the influence on choosing the right equipment for underwater scour monitoring applications. Despite the limitations in the available commercial systems to perform scour monitoring in deep water applications, green laser can prove to be advantageous where favorable water conditions exist. The limitations of using laser sensor for scour monitoring will likely to become minimal in the context of ever-expanding list of bathymetric sensors in the market.

7 REFERENCES

(1) R.L. Frizzell, L. W. Zevenbergen & R. Navarro, "Stream Channel Restoration at Bridge Sites." In *Critical Transitions in Water and Environmental Resources Management*, pp. 1-9, World Water and Environmental Resources Congress, Salt Lake City, Utah, United States, June 27-July 1, 2004.

(2) R. Joy, M.C. Jones, D. Otter, & L. Maal, *Characterization of railroad bridge service interruptions* (No. DOT/FRA/ORD-13/05). United States. Federal Railroad Administration. Office of Research and Development, Washington, D.C., 2013.

(3) B. W. Melville & S. E. Coleman, *Bridge Scour*. Water Resources Publication, Highlands Ranch , Colorado 80163, USA, 2000.

(4) L.J. Prendergast and K. Gavin. "A review of bridge scour monitoring techniques." *Journal of Rock Mechanics and Geotechnical Engineering*, 6.2: 138-149, 2014.

(5) E.V. Richardson and S. R. Davis, *Evaluating scour at bridges*. Rep. No. FHWA-IP-90-17, Hydraulic Engineering Circular No. 18 (HEC-18), Federal Highway Administration, U.S. Dept. of Transportation, Washington, D.C., 1995.

(6) M.K. Khan, M. Muzzammil, & J. Alam, "Bridge Pier Scour: A review of mechanism, causes and geotechnical aspects." *Proceedings of Advances in Geotechnical Engineering*, Aligarh, India, April 8-9, 2016.

(7) U. Kothyari, A. Kumar & R. Jain, "Influence of Cohesion on Riverbed Scour in the Wake Region of Piers." *Journal of Hydraulic Engineering*. 140. 1-13, 2014.

(8) S. Dey & R. Rajkumar, "Scour of gravel beds at bridge piers and abutments." *Proceedings of The Institution of Civil Engineers-Water Management*, pp 157-162. 2005.

(9) B.E. Hunt, "Establishing a scour monitoring." In *Erosion of Soils and Scour of Foundations* pp. 1-11, Geo-Frontiers Congress, Austin, Texas, Jan 24-26, 2005.

(10) M. Fisher, S. Atamturktur, & A.A. Khan, "A novel vibration-based monitoring technique for bridge pier and abutment scour." *Structural Health Monitoring*, 12(2), 114-125, 2013.

(11) S. Umeda, T. Yamazaki & M. Yuhi, "An Experimental Study of Scour Process and Sediment Transport around a Bridge Pier with Foundation." In *Scour and Erosion*, pp. 66-75, International Conference on Scour and Erosion (ICSE-5), San Francisco, California, November 7-10, 2010.

(12) M. Smith, D. Vericat & C. Gibbins, "Through-water terrestrial laser scanning of gravel beds at the patch scale." *Earth Surface Processes and Landforms*, 37(4), 411-421, 2012.

(13) S. Plenner, *Development and application of a simple terrestrial laser scanner*. Master thesis report, The University of Iowa. Iowa City, IA, 2014.

(14) R. Hodge, J. Brasington, & K. Richards, "In-situ characterization of grain-scale fluvial morphology using Terrestrial Laser Scanning." *Earth Surface Processes and Landforms*. 34. 10.1002/esp.1780, 2009.

(15) G.C. Guenther, A.G. Cunningham, P.E. LaRocque & D.J. Reid, "Meeting the Accuracy Challenge in Airborne LiDAR Bathymetry." *EARSel proceedings*, 27 p, Dresden, Germany, 16-17 June 2000.

(16) D.F. Maune & A. Nayegandhi, *Digital Elevation Model Technologies and Applications: The DEM User's Manual*, 3rd Edition. American Society of Photogrammetry and Remote Sensing Press, Bethesda, Maryland, 2017.

(17) H.R. Gordon & A.W. Wouters, *Some relationships between Secchi depth and inherent optical properties of natural waters*. Applied Optics, 17(21), 3341-3343, 1978.

(18) Environmental Protection Agency, *5.5 Turbidity. In Water: Monitoring & Assessment*. Retrieved from https://archive.epa.gov/water/archive/web/html/vms55.html, (Last Accessed: 08/07/2020), 2020.

(19) R. Brown, "Relationships between suspended solids, turbidity, light attenuation, and algal productivity." *Lake and Reservoir Management*, 1(1), 198-205, 1984.

(20) V.E. Brando, J.M. Anstee, M. Wettle, A.G. Dekker, S.R. Phinn & C. Roelfsema, "A physics based retrieval and quality assessment of bathymetry from suboptimal hyperspectral data." *Remote Sensing of Environment*, 113(4), 755-770, 2009.

(21) S. Nagarajan, M. Arockiasamy, & M. Banyhany, "Bridge Pier Scour Hole Simulation and 3D Reconstruction Using Green Laser (No. 18-05495)." *Compendium of Transportation Research Board 97th Annual Meeting*, Washington D.C., Jan 7th-11th, 2018.

(22) S. Moafipoor, S. Nagarajan, L. Bock & J. Fayman, "Development of Mini-UAV Based Mobile Mapping System." *Proceedings of ION GNSS+ 2014 Conference*, September 8-12, 2014, Tampa, Florida, 2014.

(23) R. Ettema, G. Constantinescu & B. Melville, B., *Evaluation of bridge scour research: Pier scour processes and predictions.* Transportation Research Board of the National Academies, Washington, D.C., 2011.

(24) E.V. Richardson & S.R. Davis, *Evaluating scour at bridges*, Fourth Edition. Federal Highway Administration, Washington D.C., 2001.

(25) B.W. Melville, "Pier and abutment scour: integrated approach." *Journal of hydraulic Engineering*, 123(2), 125-136, 1997.

(26) E.V. Richardson, J.L. Briaud, & S.J. Buchanan, "Praktische Berechnungen zu Kolken an Brücken in den USA/United States Practice for Bridge Scour Analysis." *Empfehlungen zur Anwendung von Oberflächendichtungen an Sohle und Böschung von Wasserstraßen*, (85), 71-97, 2002.

(27) Environmental Protection Agency., https://archive.epa.gov/water/archive/web/html/vms55.html. Date Accessed: 07/18/2019, 2019.

(28) J. Hand, *Typical Water Quality Values for Florida's Lakes, Stream, and Estuaries*. Florida Department of Environmental Protection, Tallahassee, FL 32399, 2004.

(29) Office for Coastal Management, *2020: 2017 NOAA NGS Topobathy Lidar: Fort Lauderdale to Miami (FL),* https://inport.nmfs.noaa.gov/inport/item/56036

(30) Florida Department of Transportation, *2018 Orthophoto*, Data source: https://ca.dep.state.fl.us/arcgis/rest/services/Imagery/Aerial_Imagery_2018/ImageServer, 2018.

(31) T. Schenk & B. Csathó, "Fusion of LIDAR data and aerial imagery for a more complete surface description." *International Archives of Photogrammetry Remote Sensing and Spatial Information Sciences*, 34(3/A), 310-317, 2002.

(32) J.D. Paul, W. Buytaert & N. Sah, "A Technical Evaluation of Lidar-Based Measurement of River Water Levels." *Water Resources Research*, 56(4), e2019WR026810, 2020.